Modelling of Masonry Infill Walls With and Without Openings

McGinley, W. Mark[1] and Nemati, Farid[2]

ABSTRACT

Masonry infill wall systems are commonly used in building construction throughout the world. The presence of the infill wall can significantly increase the stiffness of the structural system, resulting in the reduction of structure's natural period and its ductility. In some cases, the infill wall will impart large shear loads on the frame members, causing premature failure of these elements. Accurately predicting frame-infill panel interaction is therefore essential to ensure satisfactory behavior of these systems under high seismic loading and reduce risk. Research was undertaken to develop a model that can provide an accurate prediction of masonry infill wall behavior. As part of this research, a new macro-element for modeling the in-plane behavior of masonry infill walls was developed. This element combines a corner-hinged rectangular frame made of rigid bars with nonlinear spring elements to address the lateral in-plane response of the unreinforced masonry walls surrounded by structural frames. Through spring load-deformation relationships derived from expected material performance, the model is designed to predict the flexural, diagonal shear, and sliding shear response of infill masonry walls, as well as the frame-wall interaction. The nature of the proposed element also accommodates the modeling of perforated masonry walls and the effects these openings have on the performance of the infill masonry walls. The model was shown to be able to predict the behavior of unreinforced infill masonry walls with acceptable levels of accuracy.

KEYWORDS: *infill wall, macro-model, masonry, nonlinear analysis*

INTRODUCTION

Unreinforced masonry infill wall systems are used throughout the world and many of the buildings constructed in United States prior to 1950 incorporate unreinforced masonry walls within structural frames. South and Central America, North Africa and Southern Europe (both old and new) also use unreinforced masonry infill walls. However, about 40% of the buildings identified as high-risk and vulnerable to seismic damage were classified as concrete frames with masonry

[1] Professor, Department of Civil and Environmental Engineering, University of Louisville, Louisville KY, 40292, USA, m.mcginley@lousiville.edu.
[2] Former Ph. D. Student, Department of Civil and Environmental Engineering, University of Louisville, Louisville KY, 40292, USA, f0nema01@cardmail.louisville.edu.

infill shear walls [1]. The presence of masonry infills can significantly increase the stiffness of the structural system, resulting in the reduction of structure's natural period and its ductility [2]. Infill walls can also induce significant shear loads on frame members, often causing premature failure of these elements [3]. Accurately predicting frame-infill panel interaction is therefore essential to ensure satisfactory behavior of these systems under high seismic loading and reduce risk [4].This paper summarizes a portion of an investigation whose objective was to develop a numerical model that can accurately predict the masonry infill wall behavior.

PREVIOUS RESEARCH ON MASONRY INFILL WALL MODELS

In –plane Masonry Wall Micro-models
Micro-modelling is one of the most commonly used approaches for modeling a masonry infill wall. In the simplified micro-modeling, units are represented by expanded continuum elements, while the joints and unit-mortar interface are lumped together in discontinuous elements at mid-thickness of mortar layers [5] and [6]. These models have shown to be accurate in predicting localized behavior of masonry walls [6], but are computation intense and require detailed material models. In addition, to study nonlinear behavior of masonry walls and achieve accurate assembly behavior prediction, very fine meshes and detailed material models that account for non-homogeneity must be used [7]. Moreover, simplified micro-models, while accurate in the linear range, can be quite inaccurate in the nonlinear range (likely because of the large ratio of unit to mortar stiffness) [7].

In-Plane Masonry Wall Macro-models
With macro-models, the individual elements of the masonry assembly are not modelled; instead they are merged into a homogeneous anisotropic material. Thus element mesh generation does not need to reflect the actual configuration of the units and mortar in the infill masonry wall, significantly lowering computational effort.

A number of researchers have investigated the behavior of the infilled frames under in-plane loading, and many have proposed use of diagonal struts to capture the effects of infill walls [8], [9], [10]-[13], [4]. However, single compressive strut models were shown to have difficulty in describing the flexural moments and shear forces created in the frame members and they did not accurately address all aspects of the interaction between the frame and the infill [14], [15] [16], [17], [4].

To model the interaction between frame and infill more precisely, a multiple strut model for infill walls was proposed [18]. Multiple strut models were also proposed by other researchers [19], [20]. However Crisafulli found that even the most complicated multiple-strut model was not capable of describing the response of the infilled frame systems when horizontal shear sliding occurs in the masonry panel [21]. Although these models were modified further, they did not accurately predict bending moments and shear forces in the surrounding frame [22].

In light of the deficiencies described previously, there appears to be a need for an analytical model that is able to accurately predict the behavior of infill masonry wall and structural frame systems, especially with openings.

PROPOSED MODEL

To address some of the shortcomings of the models described previously, a new macro-element for masonry infill walls was developed. This element is based on the element developed by Caliò et al. [23] [24]. Caliò developed a rigid bar macro element with a series of springs used to capture flexural behavior and a set of diagonal springs to model shear behavior of masonry shear wall elements.

Figure 1 shows the proposed masonry infill wall element. This macro-element extends the element developed by Caliò to include the frame-wall interaction using gap elements at various points along the frame-infill wall interface. In addition, a total of ten shear springs (instead of the two used by Caliò) are used to better model the actual shear behavior of the masonry shear wall (especially with openings), and simulate the softening of the masonry (cracking) wall under in-plane load. A sliding shear spring is also added to address wall base failure and slip between elements. Finally, a gap element was added to simulate the interaction of the wall and frame.

(a) Shear Behavior	**(b) Flexural Behavior**
(c) Sliding Behavior	**(d) Effect of Gap Elements**
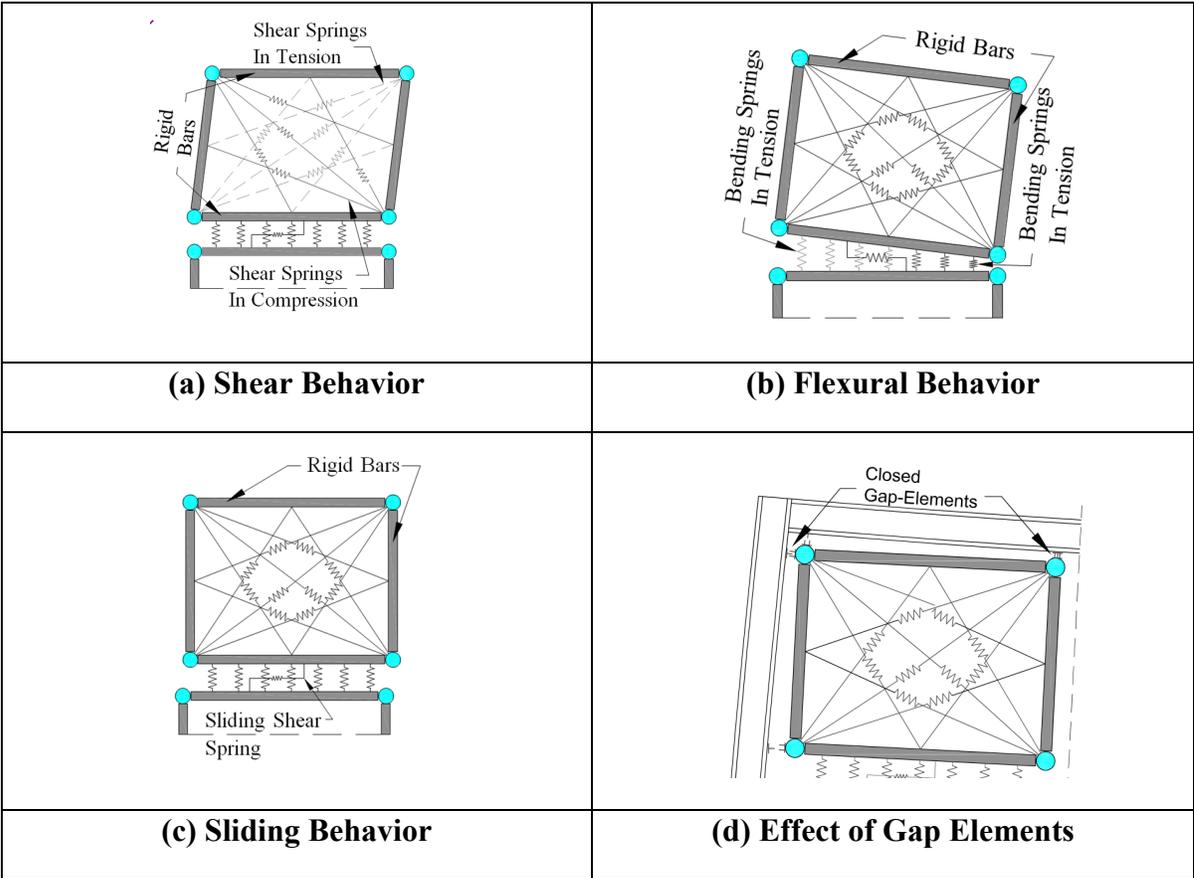
Figure 1: Proposed Macro-element (based on a similar figure in Caliò et al. [24])

The proposed macro-element consists of four rigid bars, hinged at their ends, forming a rectangular chassis to which three groups of nonlinear springs are attached. Ten nonlinear shear springs are connected at the joints and at mid-length of the rigid bars. The additional shear springs of the proposed model are used to better simulate the degradation of the shear stiffness and to address wall behavior around openings. In addition, there are groups of zero-length nonlinear springs attached perpendicularly to the rigid bars of adjacent elements. These zero-length flexural springs are used to simulate the in-plane flexural behavior of wall sections. The number of flexural springs is chosen to better simulate the gradual degradation of the flexural stiffness of the element and to account for the presence of reinforcement. Finally, nonlinear rigid-plastic links are used to connect the parallel chasses along their common edge, modelling the shear transfer between macro-elements. The constitutive relations for each group of springs, along with their calibration procedures are described later in this paper and are based on simple behavior models and masonry structural design code [25]. A more complete description of the behaviour of both the flexural and shear spring is included in the work by Nemati [26].

Figure 2 shows the typical stress-strain behavior adopted for the masonry in the proposed model and is typical for low tension strength materials (such as concrete and masonry). The masonry was assumed to have the same initial elastic moduli in both tension and compression regions [27]. A nonlinear model for the masonry is shown by the thick dashed line in Figure 2. The model defines the initial response of masonry as linear elastic up to a proportional limit. After this limit, the elastic modulus is reduced to simulate the 50% reduction in elastic modulus at peak load. This reduction is kept consistent until a second strain limit, ε_2, is reached. After this strain limit is exceeded, the effective stiffness of masonry was assumed to fall off rapidly until a final strain is reached where the stiffness is essentially zero, defining a tri-linear material model for compression. More detail on this model is included in the work by Nemati [26].

This base material model is used for the flexural springs in compression and also formed the basis for the response for the shear springs under compression loads. In tension, the same initial elastic modulus was used. The tensile strength of the flexural springs was assumed to be 10% of compressive strength, following the experimental tests by others [27]. See further discussion by Nemati [26].
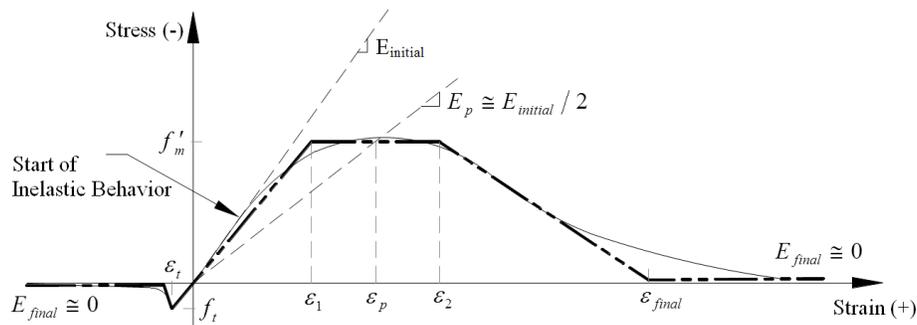
Figure 2: Simplified Isotropic Material Model for Diagonal Shear and Flexural Springs.

The initial elasticity modulus of the masonry assembly is defined as the elastic modulus of the masonry assembly in compression, E_m. This value can be obtained from masonry compression tests, or set equal to the value defined by the masonry structural design code [25]. For concrete masonry the code defined value was taken as $E_m = 900 \, f_m'$.

As described by the masonry code, the modulus of rigidity (shear modulus) was assumed to be 40 percent of the elasticity modulus [25].

To keep the modeling simple, the stiffness of the shear springs in compression was modelled in a manner similar to that of flexural springs, but with a 60% reduction in effective stiffness.

The maximum allowable shear stress in reinforced masonry shear wall elements described in the MSJC Masonry Design code [25] (with no shear reinforcing) is shown in Equation 1 below. In the proposed model, it was conservatively assumed that this limit defined the elastic shear limit beyond which the macro-element will become inelastic.

$$F_{vm} = \frac{1}{2}\left[\left(4 - 1.75\left(\frac{M}{Vd}\right)\right)\sqrt{f_m'}\right] + 0.25\frac{P}{A_n}$$

(1)

This equation can be simplified further by conservatively assuming no axial stress and an *M/Vd* ratio set to the largest possible value (1.0) defined by the MSJC code.

The average shear stress is then assumed equal to this stress, by which, an angular (shear) peak shear strain, γ_{vm}, (tensile shear) was derived.

In an effort to capture masonry infill wall shear friction behavior, two sliding shear springs were located at adjacent macro-element borders and the base of the wall. For unreinforced masonry walls, the sliding shear springs are assumed to exhibit a rigid-plastic behavior. Using a Mohr-Coulomb approach with a material cohesion strength, a coefficient of friction and a normal stress state, the ultimate shear resistance of an interface subject to shear forces was modelled [28].

In the proposed macro-element, it was initially assumed that each of the sliding shear springs has a known and near infinite stiffness. At each increase in load, the internal force in these springs was determined from equilibrium. When shear force was excess of the sliding strength, the stiffness of the sliding shear springs was reduced to near zero to simulate a sliding response with a constant resistance.

The final innovation in the proposed model is the simulation of the frame-wall interaction using gap elements. These gap elements are only used at joints of the element rigid bars adjacent to the frame members. The gap elements are connected perpendicularly to the frame members at the element joints, providing deformation compatibility between the shear wall elements and frame. These gap elements are modelled as having resistance in compression only and computationally

address the frame-infill contact problem by adding Lagrange Multipliers to the vector of unknowns.

NUMERICAL EXAMPLES

In order to evaluate the accuracy of proposed analytical model, three unreinforced masonry infill shear wall tests conducted by Dawe et al, [29] were analyzed using the proposed macro-model. The three wall tests (see Figures 3 , 4 and 5) included a solid unreinforced masonry infill wall (WA4) with no gaps in top or sides of the wall), a wall with a central opening in the infill wall (WC3), and a infill wall with and opening off center (WC5). The surrounding steel frame used AISC Metric W250 x 58 stel wide flange sections for the columns and a W200 x 46 wide flange for the beam. The masonry infill walls were constructed of ASTM C 90, 200 x 200 x 400 mm hollow concrete masonry units. Additional information on the specimen construction can be found in Dawe et al [29]. Each of the wall specimens were loaded monotonically under displacement control and the response of the specimens measured at each load step. Note that the deformation of the steel frame was limited to keep the frame response in the elastic range and allow its reuse.

To determine the material properties for use in the analysis, the initial elasticity modulus of each of the masonry infill wall models was derived from the measured initial stiffness of the infill walls since masonry assembly tests were not reported. After the initial wall stiffness was used to determine a masonry assembly elastic modulus, E_m, this modulus was then used to estimate the specified masonry assembly compression strength (f'_m). This strength was then used to derive the shear stiffness, and stress and strain end points for the macro models, as described previously.
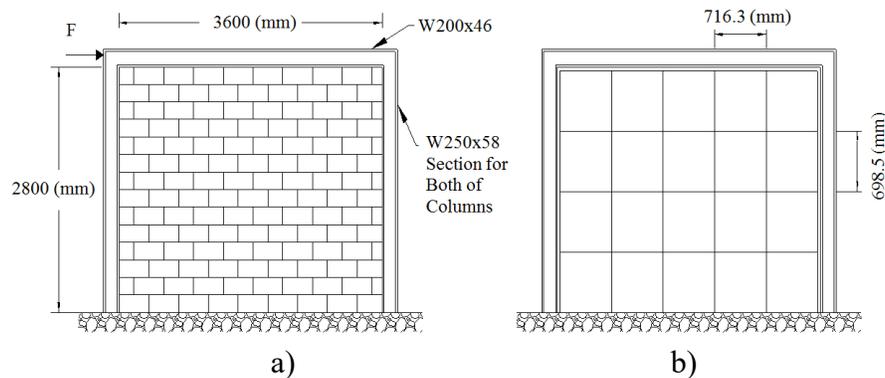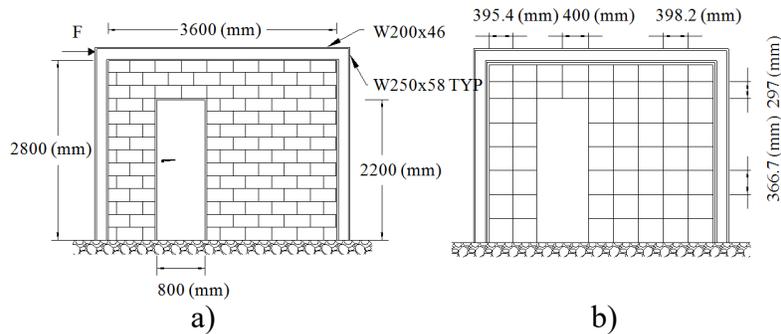

Figure 3: Specimen WA4: (a) Experimental Configuration (Solid Wall) [29]; (b) Macro-Model (NTS)

Published material properties for the wide flange shapes were used for the steel frame members in the macro-models. The steel members remained fully elastic for all analyses conducted in this investigation, and were consistent with the testing program.
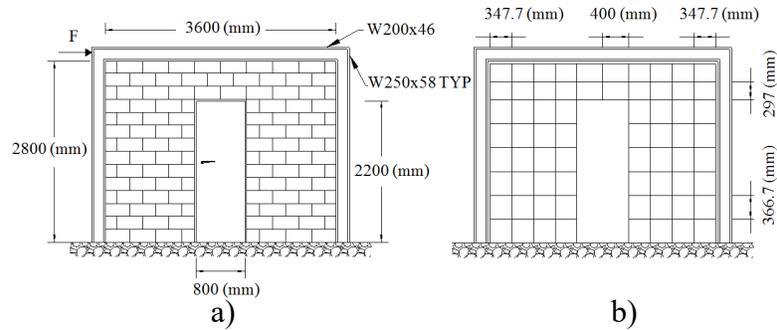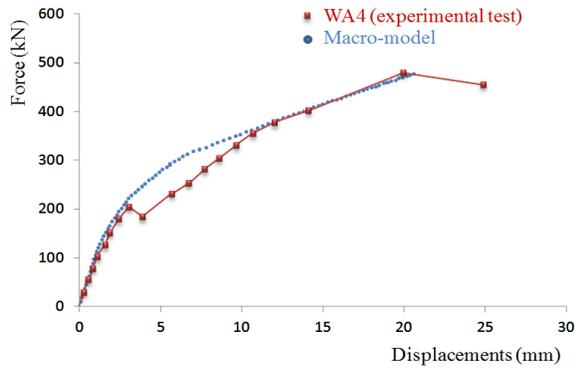
Figure 4: Specimen WC3: (a) Experimental Configuration (Central Door Opening) [Dawe et al. 1989]; (b) Macro-Model For Infill Wall With Central Opening (NTS)
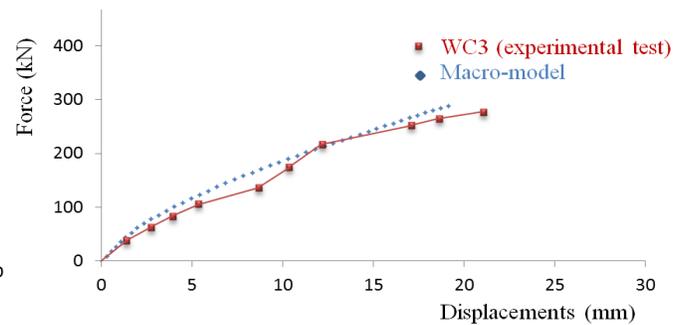

Figure 5: Specimen WC5: (a) Experimental Configuration (Door Opening Offset Towards the Loaded Side) [29]; (b) Macro-Model For Infill Wall With Offset Door Opening (NTS)

A monotonic pushover analysis was conducted on each of the models using the macro element meshes shown in Figures 3, 4 and 5, and the material models and analysis approach described earlier. The macro element mesh for each infill wall was determined by keeping the number of the macro-elements small while maintaining approximately a square aspect ratio. The mesh was varied until little difference was seen with successively finer meshes. Good results were achieved when the element meshing for perforated infill walls was such that at least two macro elements are placed along between the opening and the frame. Note that finer meshes (more than two between wall and frame) did not appreciably change the predicted wall performance.

Figures 6 through 8 show the comparison of the force-displacement response predicted for each macro-model and those obtained experimentally for infill wall Specimens WA4, WC3 and WC5. Examination of these results shows that the macro-model was able to predict the force-displacement response of the tested walls with reasonable precision. The ultimate loads for all three models are predicted within a maximum error of 1.82 % (for Specimen WC5). The displacement at the peak loads for Specimen WA4 and WC5 showed good agreement but the prediction of Specimen WC3 indicated a larger error (9 %). Examining the measured behavior of Specimen WC3 shows what appears to be a significant reduction in stiffness just prior to the ultimate load. A much better agreement between measured and predicted behavior was shown for loads just below the peak loading point.

Force (kN)

600
500
400
300
200
100
0

■ WA4 (experimental test)
● Macro-model

0   5   10   15   20   25   30

Displacements (mm)

Force (kN)

400
300
200
100
0

■ WC3 (experimental test)
● Macro-model

0   5   10   15   20   25   30

Displacements (mm)

Figure 6: Solid Wall Specimen WA4Experimental [29] vs. Macro-Model
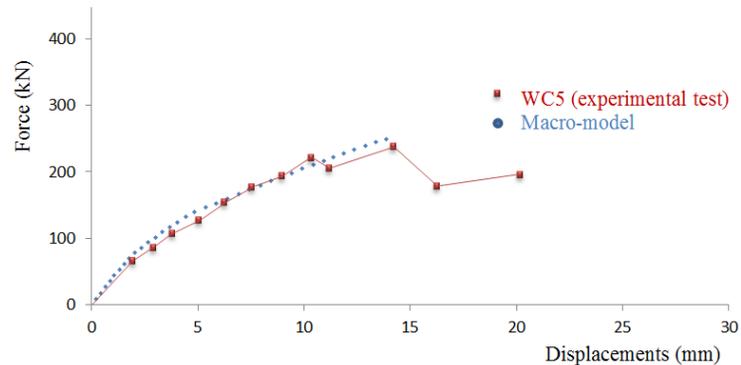
Figure 7: Wall Specimen WC3 (with Central Opening) Experimental [29] vs. Macro-Model

The analytical modelling of Specimen WA4 predicted a tensile cracking on the lower left side of the wall to occur first. With increasing load, the model predicted the formation of shear tensile cracks perpendicular to the compressive diagonal of the wall. Because the infill shear wall was surrounded by the steel frame, this cracking did not produce a significant softening of the wall elements. With further increases in the load, significant tensile/shear strains were produced at the lower left of the infill wall elements and these resulted in local interface failures. At the ultimate load, the analytical model predicted a local compressive corner crushing at the lower right side of the infill wall. Shear tensile cracks, perpendicular to the compressive diagonal of the masonry shear wall, were predicted by the analytical model as the load increased, significantly reducing the infill wall element stiffness. Flexural tensile failures on the lower left side elements of the masonry infill wall were also predicted at these load levels.   During the testing of Specimen WA4, tensile shear cracks were reported and resulted in a significant reduction of the stiffness of the wall specimen. Local corner crushing on the main diagonal near ultimate load was also observed during the tests [Dawe et al 1989]. It should be noted that, WA4 showed a measured fall off of stiffness about 199 kN before recovering stiffness for later loading. This behavior was not reproduced by the model, but the model was able to predict similar locations of tensile and shear failure (cracks) to that observed and able to predicted the ultimate load and deformation within .3% and 2 %, respectively.

For Specimen WC3 (central opening), the analyses predicted an initial tensile crack to occur at a relatively low load. However, the flexural tensile cracks predicted by the model were minor and only resulted in a local element separation. Although these cracks were not observed during the testing, the major shear cracks predicted by the analysis were observed at about the same load level as predicted. At ultimate load, the analytical model, predicted a small amount of localized masonry crushing along the main diagonal compression strut (at the lower right corner of the wall). The analysis also predicted a major sliding failure in ground level of the infill wall after this crushing. Sliding was observed in the test, although the corner crushing was not. Still, there appeared to be

reasonably good agreement between predicted and measured behavior. The model predicted the ultimate load within 1.8% and deflection (at ultimate load) within 2.3%.

Figure 8: Wall Specimen WC5 (with an Offset Opening) Experimental [29] vs. Macro-Model

The analysis of Specimen WC5 (offset opening) predicted a major flexural tensile crack to form of the lower left side of the infill wall (the section adjacent to the loaded column). The model predicted that this crack would be followed by diagonal shear crack in the infill wall, on the right side of the opening (about ½ way up the pier). With increasing loads tensile shear cracks were predicted to occur on the right side of door opening, along with a local element separation failure on the left side (at the base of the pier). It is interesting to note that the analytical model did not predict shear failure on the wall section on the left side of the door opening but did predict that, just before the ultimate load, minor corner crushing would occur in the lower right corner of the wall section to the left of the door opening. It appears that the pier to the left of door opening acts primarily in flexure. This behavior was similar to that observed in the WC5 wall test. In this test, sliding failure similar to that predicted by the model was reported. In addition, some minor diagonal cracks were also reported in the pier to the right side of the opening. In general, the proposed macro-model was able to capture the failure modes and sequence observed in the experimental tests and was able to predict the ultimate load and the displacement at with an acceptable degree of accuracy.

Thus, the proposed macro element and modeling procedure appears to be able to capture the behavior of both solid and perforated masonry infill walls. Although all examples evaluated here are unreinforced masonry infills, the macro-element is also capable of modeling infill wall reinforcement. The authors are currently expanding the macro-model to address reinforced masonry infill walls. This work will be reported later.

CONCLUSION

Unless detailed specifically to prevent interaction, masonry infill walls will affect the in-plane strength and stiffness of the structural frames, especially under lateral loading. The presence of the infill wall significantly increases the in-plane stiffness of the structural system, resulting in reduction of the structure's natural period and ductility. Although many models have been created

to study the behavior of infilled frames, most of them lack the ability to accurately model the perforated masonry infill walls. Thus, an analytical model capable of predicting the behavior of both solid and perforated unreinforced masonry walls is needed and the subject of this investigation.

The proposed macro element for masonry infill walls uses a chassis of rigid bars that anchor three different sets of nonlinear springs. These springs are used to model, tensile cracking, progressive shear failure, corner crushing due to flexural compression and sliding shear failure. In addition, the model uses a simple material model that can be easily calibrated using basic assembly tests and/or structural design code based masonry strengths.

When the proposed macro elements and modelling procedures were applied to three full-scaled infill-wall tests that contained unreinforced masonry infill walls with and without openings, there was very good agreement between predicted and observed experimental behavior.

REFERENCES

[1] T. Bashandy, N. R. Rubiano and R. E. Klingner , "Evaluation and Analytical Verification of Infilled Frame Test Data.", PMFSEL Report 95-1, 1995.

[2] W. W. El-Dakhakhni, M. Elgaaly and A. A. Hamid, "Finite element modeling of concrete masonry infilled steel frame.", *Proc., 9th Canadian Masonry Symposium*, Ottawa, Canada, 2001.

[3] FEMA, "FEMA 310. (1998). Handbook for the Seismic Evaluation of Buildings", Federal Emergency Management Agency, Washington, D.C., 1998.

[4] P. Asteris, "Lateral Stiffness of Brick Masonry Infilled Plane Frames.", *J. Struct. Eng.,* Vols. J. Struct. Eng., 10.1061/(ASCE)0733-9445(2003)129:8(1071), 2003.

[5] P. B. Lourenco, P. Roca, C. Modena and S. Agrawal, "Homogenization Approaches for Structural Analysis of Masonry Buildings.", *Struct. Analysis of Historical Constructions. Proc., The 5th International Conf.*, LNew Delhi, India, 2006.

[6] G. Grecchi, "Material and structural behavior of masonry: simulation with a commercial code.", Laurea Thesis, University of Pavia., Lombardy, Italy., 2010.

[7] A. Zucchini and P. Lourenço, "A micro-mechanical model for the homogenization of masonry.", *Int. J. of Solids and Structures,* vol. 39, p. 3233–3255, 2002.

[8] S. V. Polyakov, "On the interaction between masonry filler walls and enclosing frame when loading in the plane of the wall.", Translation in Earthquake Engineering, Research Institute (EERI), San Francisco., 1960.

[9] B. S. Smith, "Behavior of Square Infilled Frames.", *Journal of the Structural Division, ASCE, Vol. 92, No.1, pp. 381-404,* vol. Vol. 92, no. No.1, pp. pp. 381-404, 1966.

[10] R. Mainstone, "On the Stiffness and Strengths of Infilled Frames.", *Proc., The Institution of Civil Engineers, Supplement IV, 57-90*, London, 1971.

[11] T. Liauw and K. Kwan, "Nonlinear behaviour of non-integral infilled frames.", *Comp. and Struct.,* vol. 18, no. DOI: 10.1016/0045-7949(84)90070-1, pp. 551- 560, 1980.

[12] T. Paulay and M. J. N. Pristley, *Seismic Design of Reinforced Concrete and Masonry Buildings*, New York: Wiley, New York, 1992.

[13] R. Flanagan and R. Bennett, "In-Plane Analysis of Masonry Infill Materials.", *Pract. Period. Struct. Des. Constr.,* Vols. 0.1061/(ASCE)1084-0680(2001)6:4(176), p. 1084, 2001.

[14] J. Reflak and P. Fajfar, "Elastic analysis of infilled frames using substructures.", *Proc., 6th Canadian Conf. on Earthquake Engineering, University of Toronto Press*, Toronto, 1991.

[15] S. Buonopane and R. White, "Pseudodynamic Testing of Masonry Infilled Reinforced Concrete Frame.", *J. Struct. Eng.,* Vols. J. Struct. Eng., 10.1061/(ASCE)0733-9445(1999)125:6(578), 1999.

[16] A. A. Chaker and A. Sherifati, "ChaInfluence of masonry infill panels on the vibration and stiffness characteristics of R/C frame buildings", *Earthq. Eng. Struct. Dyn.,* vol. 28(9), p. 1061–1065, 1999.

[17] A. Mohebkhah, A. Tasnimi and H. Moghadam, "Modified Three-Strut (MTS) Model for Masonry-Infilled Steel Frames with Openings", *JSEE. Spring and Summer, Vol. 9, No. 1,2/ 39,* Vols. Vol. 9, No. 1,2/ 39, 2007.

[18] V. Thiruvengadam, "On the natural frequencies of infilled frames," *Earthquake Eng. Struct. Dyn.,* vol. 13(3) , p. 401–419, 1985.

[19] C. Z. Chrysostomou, P. Gergely and J. F. Abel, "A six-strut model for nonlinear dynamic analysis of steel infilled frames," *Int. J. Struct. Stab. Dyn.,,* vol. 2(3), p. 335–353, 2002.

[20] W. W. El-Dakhakhni, "Experimental and analytical seismic evaluation of concrete masonry-infilled steel frames retrofitted using GFRP laminates.", *Ph.D. thesis*, Drexel Univ., Philadelphia, USA, 2002.

[21] F. J. Crisafulli, "Seismic Behaviour of Reinforced Concrete Structures with Masonry Infills.", *PhD Thesis*, Dept. of Civil Engng., Univ. of Canterbury, New Zealand, 1997.

[22] P. Asteris, S. Antoniou, D. Sophianopoulos and C. Chrysostomou, "Mathematical Macromodeling of Infilled Frames: State of the Art.", *J. Struct. Eng.,* Vols. 10.1061/(ASCE)ST.1943-541X.0000384, 2011.

[23] I. Caliò and B. Pantò, "A macro-element modelling approach of Infilled Frame Structures.", *Computers & Structures,,* Vols. 143:91–107, DOI: 10.1016/j.compstruc.2014.07.008, 2014.

[24] I. Caliò, M. Marletta and B. Pantò, "A new discrete element model for the evaluation of the seismic behavior of unreinforced masonry buildings.", *Engng. Struct., 40 (2012) 327–338,* vol. 40 (2012), p. 327–338, 2012.

[25] Masonry Standards Joint Committtee, MSJC (Masonry Standards Joint Committee). (2013). "Building Code Requirements for Masonry Structures.", TMS 402/ACI 530/ASCE 5-2013, Longmont, CO.: TMS/ACI/ASCE, 2013.

[26] F. Nemati, "MACRO MODEL FOR SOLID AND PERFORATED MASONRY INFILL FRAMES", *Ph. D. Thesis,* University of Lousiville, Louisville, KY, 2015.

[27] H. Lotfi and P. Shing, "Interface Model Applied to Fracture of Masonry Structures.", *J. Struct. Eng.,* Vols. 10.1061/(ASCE)0733-9445(1994)120:1(63), 1994.

[28] FIB, Fib Model Code for Concrete Structures. Fédération Internationale du Béton (fib), Lausanne, Switzerland, Lausanne, Switzerland: Fédération Internationale du Béton, 2010.

[29] J. L. Dawe and C. K. Seah, "Behavior of Masonry Infilled Steel Frames.", *Canadian J. of Civil Engrng.,* vol. 16, pp. 865-876., 1989.